## SUPPLEMENTARY INFORMATION

# Dual roles of yeast Rad51 N-terminal domain in repairing DNA double-strand breaks

Tai-Ting Woo, Chi-Ning Chuang, Mika Higashide, Akira Shinohara, and Ting-Fang Wang

### Supplementary Figure S1

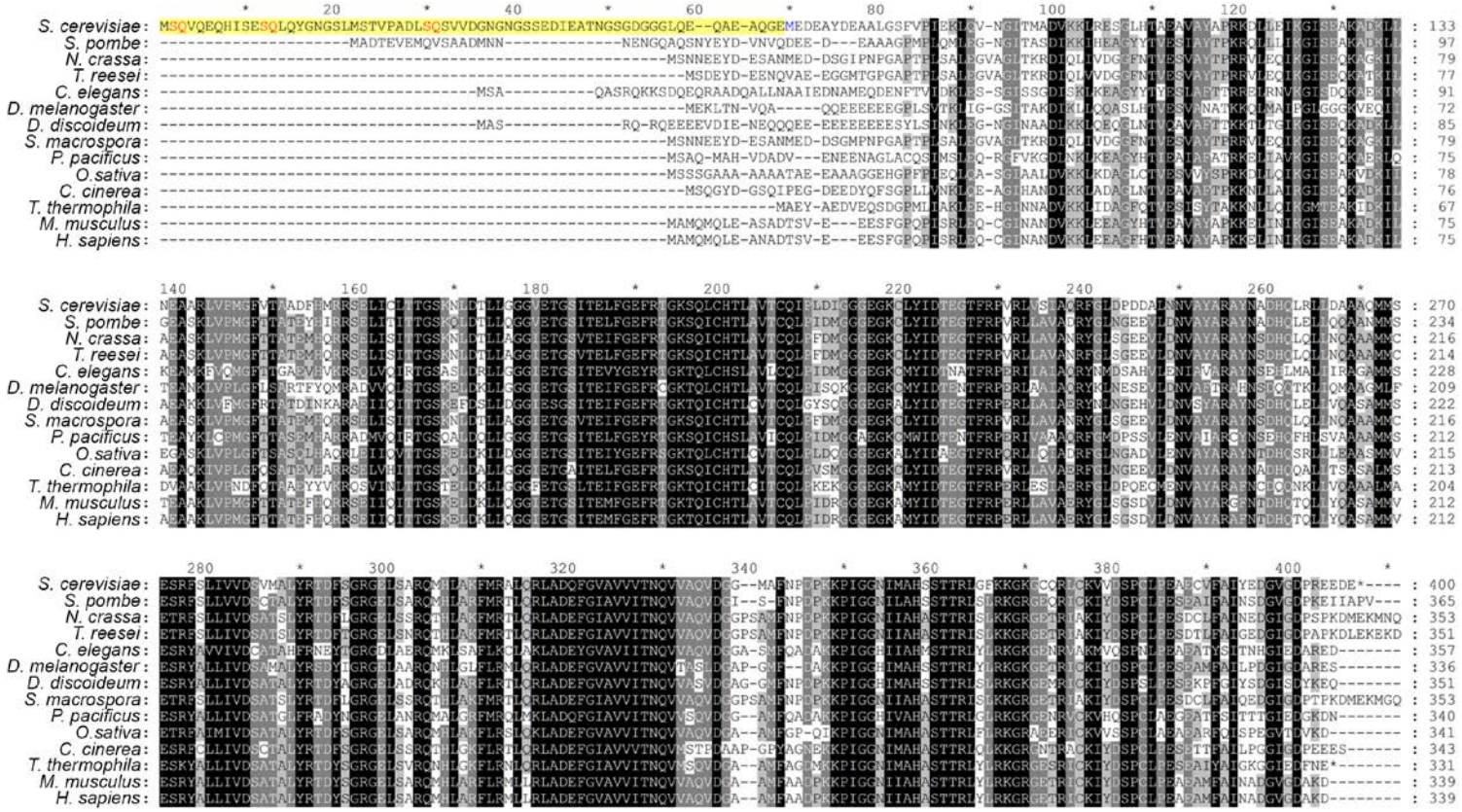


**Supplementary Figure S1.** Rad51 orthologs. The multiple sequence alignment of Rad51 orthologs from 14 eukaryotic organisms (from yeast to human) was generated using Clustal Omega (version 1.2.4). Identical residues are shaded in black. Dark grey and light grey indicate 80% and 60% conserved substitutions, respectively. The $NH_2$-terminal domain (NTD) of *S. cerevisiae* Rad51 is shaded in yellow, with the three SQ motifs comprising the putative SCD highlighted in red. The methionine ($Met^{67}$) following the NTD is shown in blue.

## Supplementary Figure S2

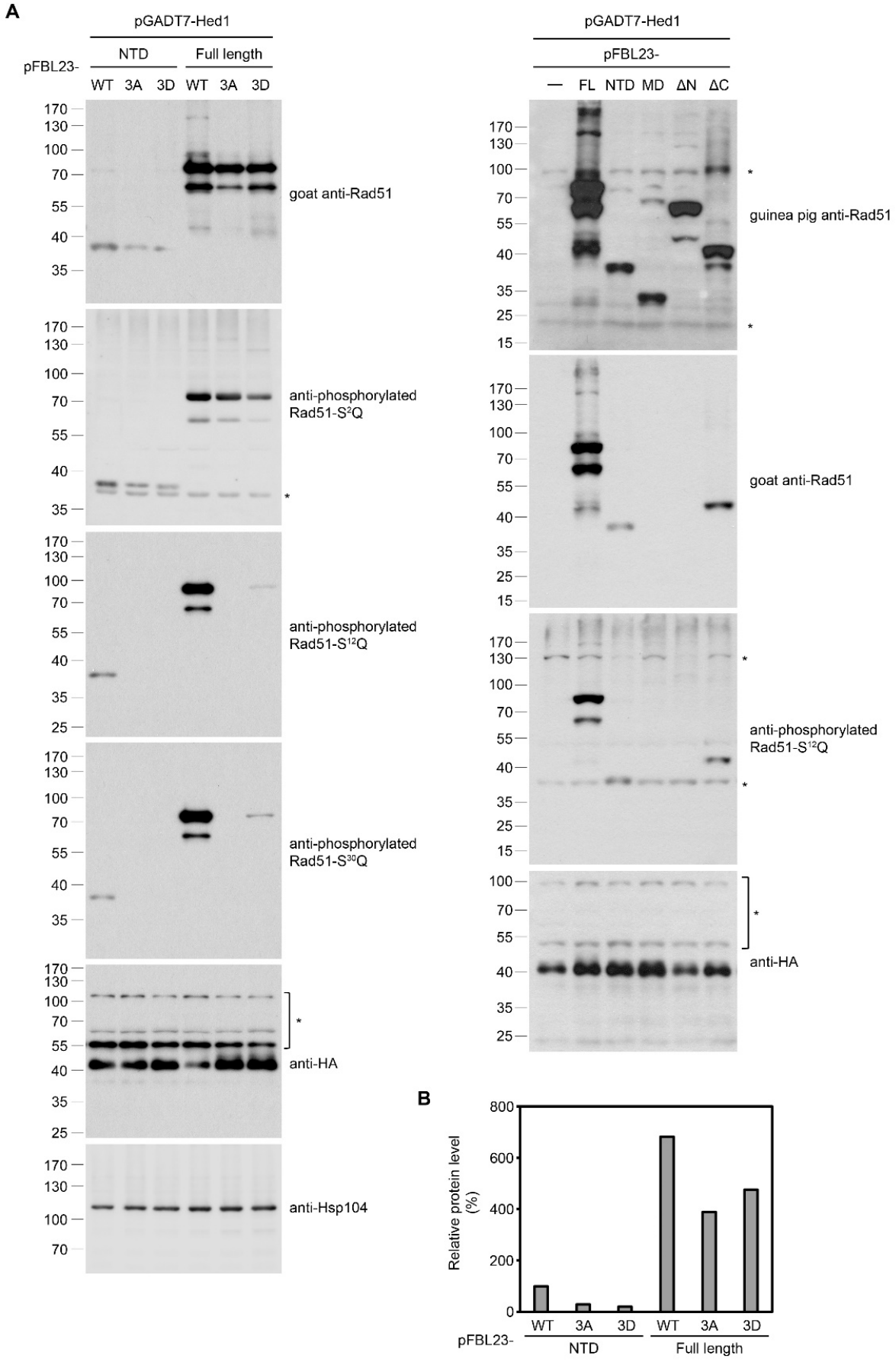

**Supplementary Figure S2.** Rad51-NTD phosphorylation of protein expression with LexA-tagging in Y2H assays**.** (**A**) Total cell lysates were prepared from reporter cells during the Y2H experiments described in Supplementary Table 3, and then visualized by immunoblotting with the corresponding antisera. The anti-HA antisera were used to confirm the expression of the HA-tagged GADT7-Hed1 fusion proteins. Asterisks indicate non-specific bands. (**B**) Quantifications of the protein bands in immunoblots detecting variants of LexA-tagged Rad51-NTD and Rad51 full-length (FL) proteins using goat anti-Rad51, normalized to Hsp104 levels using ImageJ software and shown as the relative protein levels as compared to WT Rad51-NTD-LexA expressed from the pFBL23 vector.

**Supplementary Figure S3**

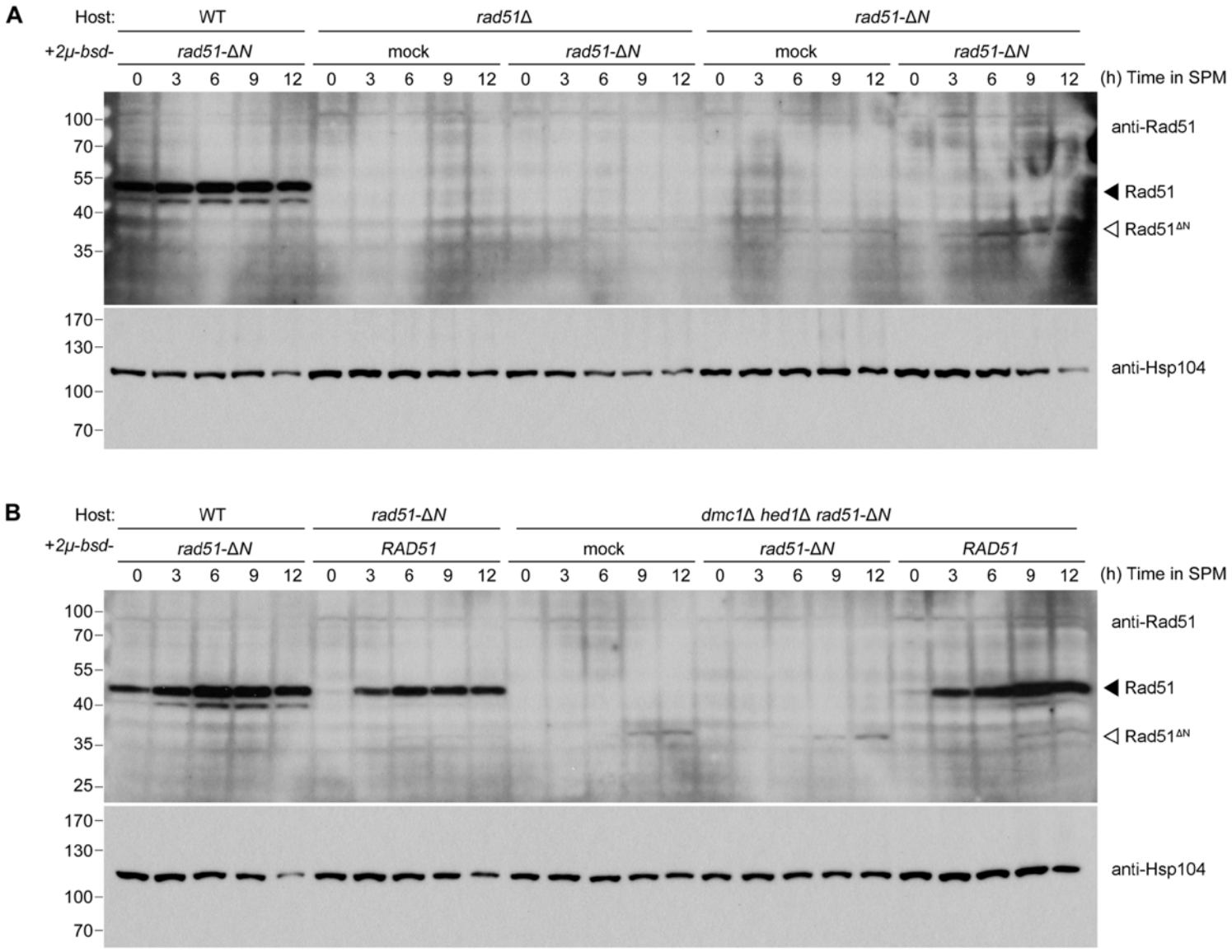


**Supplementary Figure S3.** Immunoblotting using guinea pig anti-Rad51 antisera that we used for the immunocytochemistry assay in Figure 4B and 4C. The predicted molecular weight of Rad51-ΔN is 36,270 daltons. *2μ*-based overexpression vectors carrying WT *RAD51* or *rad51-ΔN* alleles were transformed into diploid strains of indicated genotypes (see Table 2).

**Supplementary Figure S4**

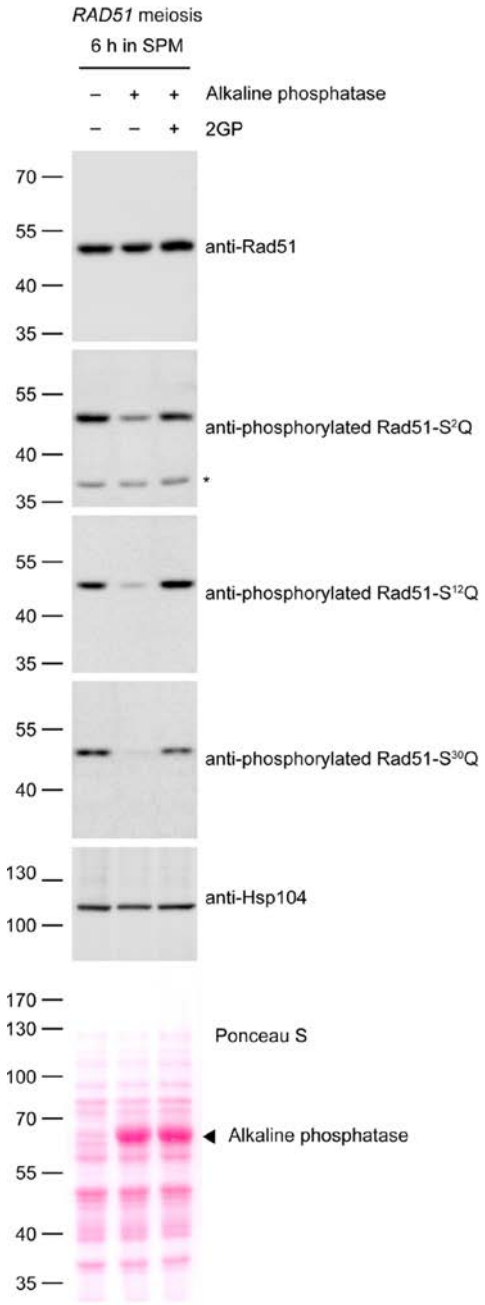


**Supplementary Figure S4.** Validation of the phospho-specific antisera against Rad51-NTD using dephosphorylation assay. Total lysates of WT meiotic cultures in SPM were subjected to *in vitro* dephosphorylation reaction (see "Materials and Methods" section) using bovine intestinal alkaline phosphatase, and then analyzed by immunoblots using corresponding antisera as described in Figure 3E. The general phosphatase inhibitor 2-glycerophosphate (2GP) was used in the negative control experiments. The presence of alkaline phosphatase (molecular weight: ~70 kDa, indicated by the black arrowhead) is visualized using Ponceau S-staining (Sigma-Aldrich) of the PVDF membrane before immunoblotting. Asterisk indicates nonspecific bands.

## Supplementary Figure S5

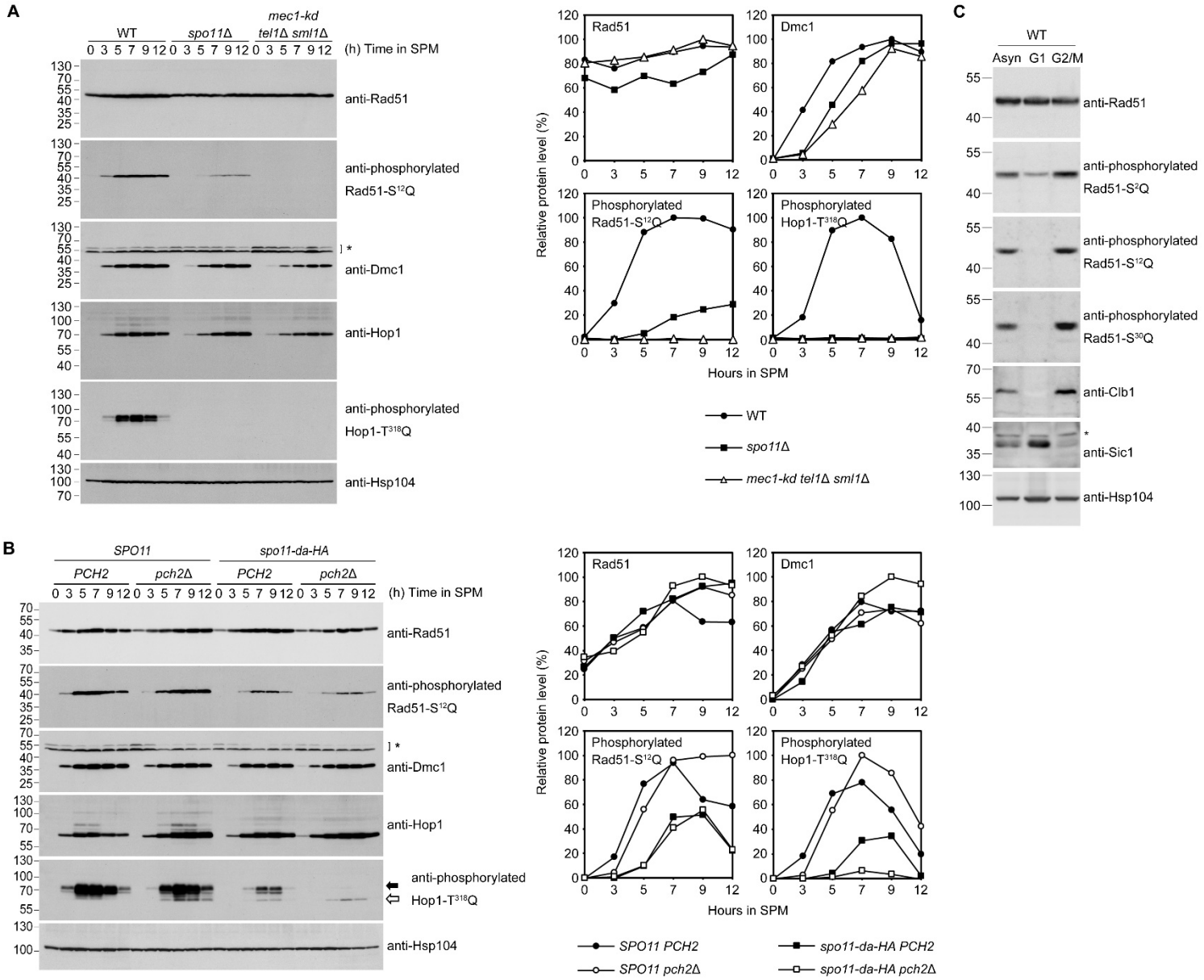


**Supplementary Figure S5.** *SPO11*-independent Rad51-NTD phosphorylation and *SPO11*-dependent Hop1 phosphorylation are differentially regulated by Pch2 when nucleus-wide DSB abundance is low. (**A, B**) Total cell lysates were prepared from indicated meiotic cells at indicated sporulation time-points as previously described (1,2), and then visualized by immunoblotting with the corresponding antisera. Hsp104 was used as a loading control. (**B**) Both hyperphosphorylated (black arrow) and hypophosphorylated (white arrow) Hop1 proteins were detected. The asterisk indicates non-specific bands. Immunoblots were quantified using ImageJ software. Plot shows protein levels normalized to Hsp104 level at that time-point. The highest level of immunoblot signal in each blot was used as the standard for comparison. (**C**) Immunoblots with indicated antisera using total cell lysates prepared from *MATa* WT

cultures of asynchronous mid-log phase (Asyn) and synchronous cultures (G1 or G2/M). To synchronize cell cycle, cells were grown to mid-log phase ($OD_{600} \approx 0.7$, harvested as Asyn) and diluted to $OD_{600} \approx 0.5$ with fresh YPD medium containing α-factor (150 μM). After 3 h treatment, synchronous G1 cells were harvested for lysates or washed twice with fresh medium and then resuspended in fresh medium containing nocodazole (15 μg/ml). Synchronous G2/M cultures were harvested after 2 h nocodazole-treatment. Clb1 is the B-type cyclin protein and appears in G2/M (3). Sic1 is the inhibitor of CDK/Clb complex in G1 phase (4). The asterisk indicates non-specific bands.

**Supplementary Figure S6**

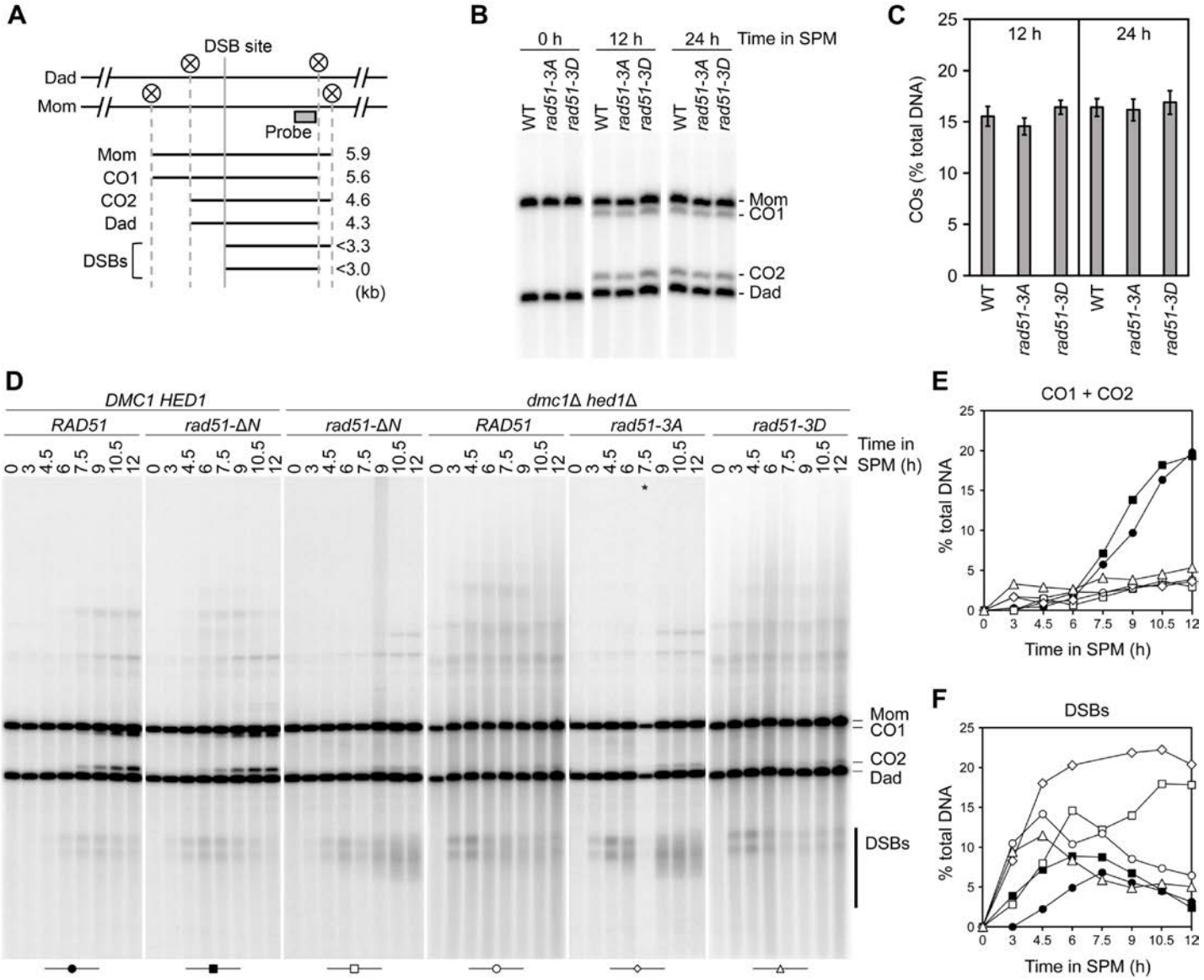


**Supplementary Figure S6.** Physical analysis. (**A**) Schematic representation of polymorphisms of XhoI restriction sites (circled Xs) at the *HIS4-LEU2* DSB hotspot and the position of the probe for detecting crossover formation (CO1 and CO2) between homologous chromosomes (represented as "Mom" and "Dad") and DSBs. (**B**) Detection of crossover products by means of Southern blot for premeiotic (0 h) and postmeiotic (12 h and 24 h) cultures of the indicated strains. One group of triplicate experiments is shown. (**C**) Quantification of (**B**). Percentages of the intensity of CO products over total hybridization signals are shown. Error bars indicate standard deviation between experiments. (n = 3) (**D**) Full time-course experiments of physical analysis for detection of crossover formation and DSB processing Southern blot results are quantified in (**E**) and **(F**), respectively, with the percentage of total hybridizing DNA signals being plotted. Asterisk, sample not included for quantification.

**Supplementary Figure S7**

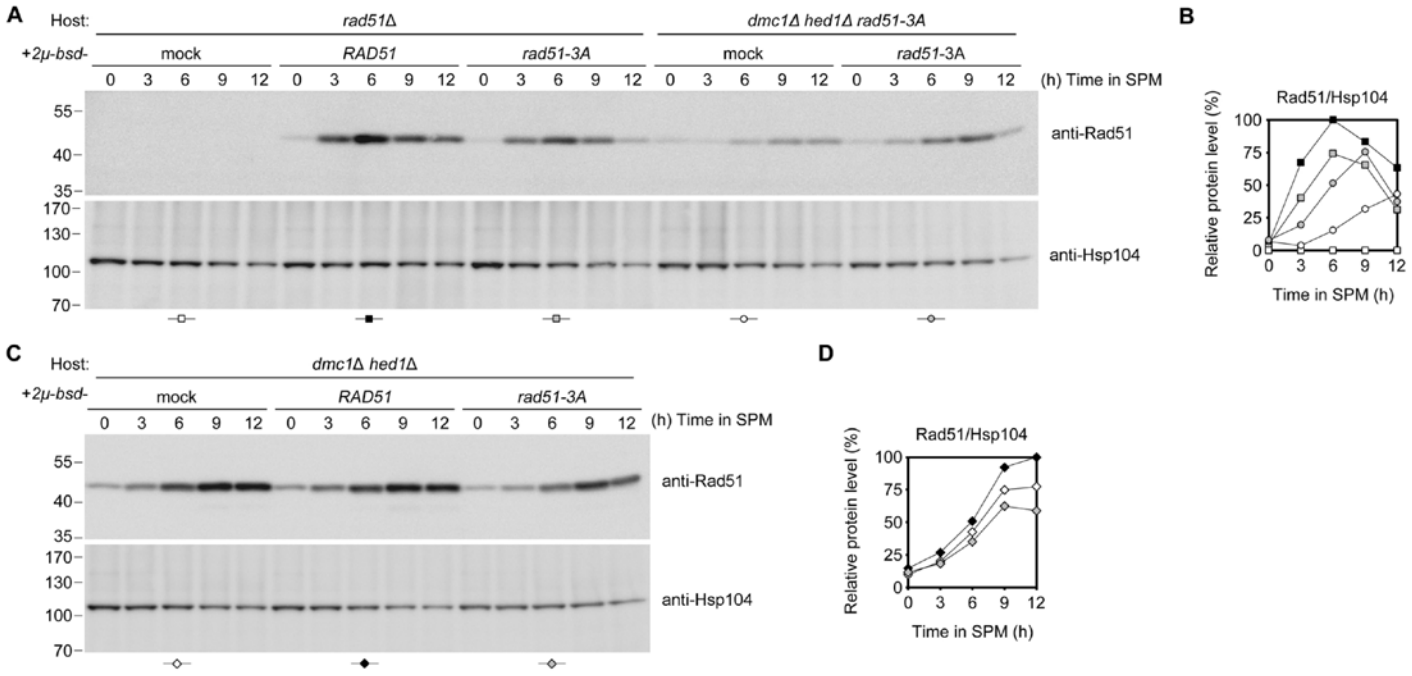


**Supplementary Figure S7**. *2μ*-based overexpression vectors carrying WT *RAD51* or *rad51-3A* alleles were transformed into diploid strains of indicated genotypes (see Table 2) and the immunoblotting time-course analyses were conducted using the indicated antibody. Rad51 protein levels normalized to Hsp104 levels in (**A**) and (**C**) are quantified and plotted in (**B**) and (**D**), respectively. The highest level of immunoblot signal in each blot was used as the standard for comparison.

**Supplementary Table S1. Plasmids used in this study**

| Plasmid number | Vector | Insert |
|---|---|---|
| pTFW2450 | pFBL23 | — |
| pTFW9901 | pFBL23 | *RAD51* |
| pTFW9903 | pFBL23 | *rad51-3A* |
| pTFW9916 | pFBL23 | *rad51-3D* |
| pTFW9946 | pFBL23 | *rad51-NTD* |
| pTFW9947 | pFBL23 | *rad51-3A-NTD* |
| pTFW9948 | pFBL23 | *rad51-3D-NTD* |
| pTFW9949 | pFBL23 | *rad51-ΔN* |
| pTFW9955 | pFBL23 | *rad51-MD* |
| pTFW9956 | pFBL23 | *rad51-ΔCAD* |
| pTFW3796 | pGADT7 | — |
| pTFW9902 | pGADT7 | *HED1* |
| pTFW8670 | pYC6/CT | *2μ* origin (replacing *CEN6/ARSH4*) |
| pTFW9884 | pTFW8670 | $P_{RAD51}$-*RAD51*-$Ter_{RAD51}$ |
| pTFW9888 | pTFW8670 | $P_{RAD51}$-*rad51-3A*-$Ter_{RAD51}$ |
| pTFW9968 | pTFW8670 | $P_{RAD51}$-*rad51-ΔN*-$Ter_{RAD51}$ |
| pTFW9957 | pYC2/NT-C | $P_{RAD51}$-LacZ-NLS-V5-$His_6$-$Ter_{CYC1}$ |
| pTFW9958 | pTFW9957 | *rad51-NTD* |
| pTFW9959 | pTFW9957 | *rad51-3A-NTD* |
| pTFW9960 | pTFW9957 | *rad51-3D-NTD* |

**Supplementary Table S2. *S. cerevisiae* strains used in this study**

| Name | Genotype | Source/reference |
|---|---|---|
| WHY2129 [a] | *MATa ho::hisG lys2 ura3 leu2::hisG arg4-bgl* | Nancy Kleckner |
| WHY2199 | *MATa/MATα ho::hisG/" lys2/" ura3/" leu2::hisG/" arg4-bgl/arg4-nsp* | Nancy Kleckner |
| WHY1192 | *MATa YCpromURA3-tetR-GFP::LEU2 CENV::336tetO-HIS3MX6 ADE2 his3::hisG trp1::hisG leu2::hisG ura3* | (5) |
| WHY3255 | *MATa/MATα YCpromURA3-tetR-GFP::LEU2/" CENV::336tetO-HIS3MX6/" ADE2/" his3::hisG/" trp1::hisG/" leu2::hisG/" ura3/"* | (5) |
| WHY3395 | as WHY3255, but *rad51Δ::kanMX4/"* | (5) |
| WHY12799 [b] | as WHY3255, but *RAD51::hphMX4/"* | This work |
| WHY12829 [b] | as WHY3255, but *rad51-S2A::hphMX4/"* | This work |
| WHY12831 [b] | as WHY3255, but *rad51-S12A::hphMX4/"* | This work |
| WHY12884 [b] | as WHY3255, but *rad51-S30A::hphMX4/"* | This work |
| WHY12885 [b] | as WHY3255, but *rad51-S2A S12A::hphMX4/"* | This work |
| WHY12959 [b] | as WHY3255, but *rad51-3A::hphMX4/"* | This work |
| WHY1762 | *MATa/MATα ho::LYS2/" lys2/" ura3/" his4B::LEU2/his4X::LEU2 arg4-bgl/arg4-nsp leu2::hisG/" cyh$^R$/CYH tel1Δ::hisG-URA3-hisG/"* | Douglas Bishop |
| WHY9047 | *MATa/MATα ura3 leu2 mec1-kd/" sml1Δ::hphMX4/"* | (6) |
| WHY9754 | as WHY9047, but *tel1Δ::kanMX4/"* | (6) |
| NHY4723 | *MATa ho::hisG leu2::hisG ura3Δ(PstI-SmaI)::hisG ERG1-(Sal1) his4-X::LEU2-(NgoMIV;+ori)-URA3* | (7) |
| NHY4763 | *MATa/MATα ho::hisG/" leu2::hisG/" ura3Δ(PstI-SmaI)::hisG /" ERG1-(Sal1)/ERG1-(SpeI), HIS4::LEU2-(BamHI; +ori)/his4-X::LEU2-(NgoMIV; +ori)-URA3* | (7) |
| NHY4765 | as NHY4763, but *dmc1Δ::kanMX4/" hed1Δ::kanMX4/"* | (7) |
| WHY12738 [c] | as NHY4763, but *dmc1Δ::kanMX4/"* | This work |
| WHY13038 [b] | as NHY4763, but *RAD51::hphMX4/"* | This work |
| WHY13350 [c] | as NHY4763, but *rad51Δ::hphMX4/"* | This work |
| WHY13435 [b] | as NHY4763, but *rad51-ΔN::hphMX4/"* | This work |
| WHY12943 [b] | as NHY4763, but *rad51-3A::hphMX4/"* | This work |
| WHY13201 [b] | as NHY4763, but *rad51-3D::hphMX4/"* | This work |
| WHY13529 [b] | as NHY4763, but *dmc1Δ::kanMX4/" rad51-ΔN ::hphMX4/"* | This work |
| WHY12972 [b] | as NHY4763, but *dmc1Δ::kanMX4/" rad51-3A::hphMX4/"* | This work |
| WHY13205 [b] | as NHY4763, but *dmc1Δ::kanMX4/" rad51-3D::hphMX4/"* | This work |
| WHY13042 [b] | as NHY4765, but *RAD51::hphMX4/"* | This work |

| | | |
|---|---|---|
| WHY13437 [b] | as NHY4765, but *rad51-ΔN::hphMX4/"* | This work |
| WHY12935 [b] | as NHY4765, but *rad51-3A::hphMX4/"* | This work |
| WHY13203 [b] | as NHY4765, but *rad51-3D::hphMX4/"* | This work |
| WHY13907 [b] | as NHY4723, but *rad51-S192A::hphMX4* | This work |
| WHY13915 [b] | as NHY4723, but *rad51-4A::hphMX4* | This work |
| WHY14007 [b] | as NHY4723, but *rad51-8A::hphMX4* | This work |
| WHY14015 [b] | as NHY4723, but *rad51-11A::hphMX4* | This work |
| WHY13534 [d] | *MATa/MATα ura3/" leu2/" sml1Δ::hphMX4/"* | This work |
| WHY13535 [d] | *MATa/MATα ura3/" leu2/" sml1Δ::hphMX4/" rad51-ΔN::hphMX4/"* | This work |
| WHY12378 [c] | *MATα ho::hisG lys2 ura3 leu2::hisG arg4-nsp BLA::His$_{10}$-SMT3 pdr5Δ::natMX4* | This work |
| WHY13997 [e] | *MATα trp1::hisG ura3 pdr5Δ::natMX4 RAD51::hphMX4* | This work |
| WHY14000 [e] | *MATα trp1::hisG ura3 pdr5Δ::natMX4 rad51-S2A::hphMX4* | This work |
| WHY14003 [e] | *MATα trp1::hisG ura3 pdr5Δ::natMX4 rad51-S12A::hphMX4* | This work |
| WHY14001 [e] | *MATα leu2::hisG ura3 pdr5Δ::natMX4 rad51-S30A::hphMX4* | This work |
| WHY13586 [e] | *MATα ura3 pdr5Δ::natMX4 rad51-3A::hphMX4* | This work |
| WHY14042 [f] | *MATa/MATα ura3/" leu2/" mec1-kd/" sml1Δ::hphMX4/" dmc1Δ::kanMX4/" hed1Δ::kanMX4/"* | This work |
| DKB490 | *MATa/MATα ho::LYS2/" lys2/" ura3/" leu2::hisG/" ade2::LK/" his4XB/his4B::ADE2-his4X spo11::hisG-URA3-hisG/"* | (8) |
| VBY1449 | *MATa/MATα ade2Δ/" can1$^R$/CAN1$^S$ met13B/MET13 trp5-S/TRP5 CENVIII::URA3/CENVIII CENIII/CENIII::ADE2 thr1-A/THR1 cup1$^S$/CUP1 HIS4/ his4-B LYS5/lys5-P CYH2/cyh2$^R$ spo11-(D290A)-HAHis6:: kanMX4/"* (mating of SKY1062 and SKY638) | (9) |
| VBY1605 | as VBY1449, but *pch2Δ::hphMX4/"* | (9) |
| WHY3285 | *MATa/MATα ho::hisG/" leu2::hisG/" ura3Δ(PstI-SmaI)/" HIS4::LEU2-(BamHI)/his4-X::LEU2-(BamHI)–URA3* | (10) |
| WHY6082 | as WHY3285, but *pch2Δ::kanMX4/"* | (10) |
| L40 | *MATa leu2 his3 trp1 ade2 GAL4 gal80 LYS2::(lexAop)4-HIS3 URA3::(lexAop)s-lacZ* | (10) |
| WHY13281 [c] | as L40, *but rad51Δ::hphMX4* | This work |

All strains except L40 and WHY13281 are in the SK1 background.

a. The laboratory standard strain used for the quantitative yeast LacZ assays.

b. The indicated *rad51* mutations were integrated into each haploid and were confirmed using DNA sequencing. The haploid mutants were then mated to make diploids.

Unless otherwise specified, haploid *rad51* mutants isogenic to WHY1192 or NHY4723 were used in vegetative MMS assays.

c. Yeast strains with PCR-based gene disruption were confirmed using Southern-blotting.

d. Yeast mutants generated by breeding haploid parental strains of WHY9047 and of WHY13435.

e. Yeast mutants generated by breeding WHY12378 and each of the indicated *rad51* mutants that are isogenic to WHY1192.

f. Yeast mutants generated by breeding haploid parental strains of WHY9047 and of NHY4765.

**Supplementary Table S3. Yeast two-hybrid analyses**

| [1]X-LexA | [1]Gal4AD-Y | β-galactosidase activity[2,3] |
|---|---|---|
| — | Hed1 | 0.2 ± 0.1 (n = 6) |
| Rad51$^{WT}$ (1-400 a.a)[4] | Hed1 | 50.5 ± 8.3 (n = 6) |
| [5]Rad51$^{3A}$ | Hed1 | 68.8 ± 10.2 (n = 3) |
| [5]Rad51$^{3D}$ | Hed1 | 56.5 ± 6.9 (n = 3) |
| NTD$^{WT}$ (1-66 a.a.) | Hed1 | 0.3 ± 0.1 (n = 6) |
| [5]NTD$^{3A}$ | Hed1 | 0.2 ± 0.0 (n = 3) |
| [5]NTD$^{3D}$ | Hed1 | 0.3 ± 0.0 (n = 3) |
| MD (67-143 a.a) | Hed1 | 0.5 ± 0.0 (n = 3) |
| ΔN (67-400 a.a) | Hed1 | 11.1 ± 4.9 (n = 3) |
| ΔCAD (1-143 a.a.) | Hed1 | 0.6 ± 0.0 (n = 3) |
| Rad51$^{WT}$ | — | 0.7 ± 0.1 (n = 6) |
| Rad51$^{3A}$ | — | 0.5 ± 0.0 (n = 3) |
| Rad51$^{3D}$ | — | 0.7 ± 0.0 (n = 3) |
| NTD$^{WT}$ | — | 0.3 ± 0.1 (n = 6) |
| NTD$^{3A}$ | — | 0.2 ± 0.0 (n = 3) |
| NTD$^{3D}$ | — | 0.2 ± 0.0 (n = 3) |
| MD | — | 0.8 ± 0.2 (n = 3) |
| ΔN | — | 0.5 ± 0.0 (n = 3) |
| ΔCAD | — | 0.7 ± 0.1 (n = 3) |

1. X-LexA: the bait protein X is $NH_2$-terminal to LexA (11,12); Hed1 is expressed from pGADT7 vectors (Clontech, USA) (13,14).
2. The two-hybrid assays were performed in a L40 *rad51*Δ reporter strain. All experiments were carried out at least three times and each time with three biological replicates.
3. One unit of β-galactosidase activity is defined as 1 μmol of o-nitrophenyl β-galactopyranoside hydrolyzed (measured with optical density at 420 nm) per min per

$OD_{600}$ (cell density measured with optical density at 600 nm).

4. The numbers refer to amino acid (a.a.) position in each bait protein X. The full-length Rad51 protein has 400 amino acid residues. Three serine residues ($S^{2}$, $S^{12}$, and $S^{30}$) were mutated into alanines (A) or aspartic acids (D) in $Rad51^{3A}$ and $NTD^{3A}$, or $Rad51^{3D}$ and $NTD^{3D}$, respectively.

## REFERENCES


1. Chuang, C.N., Cheng, Y.H. and Wang, T.F. (2012) Mek1 stabilizes Hop1-Thr318 phosphorylation to promote interhomolog recombination and checkpoint responses during yeast meiosis. *Nucleic Acids Res*, **40**, 11416-11427.
2. Cheng, Y.H., Chuang, C.N., Shen, H.J., Lin, F.M. and Wang, T.F. (2013) Three distinct modes of Mec1/ATR and Tel1/ATM activation illustrate differential checkpoint targeting during budding yeast early meiosis. *Mol Cell Biol*, **33**, 3365-3376.
3. Grandin, N. and Reed, S.I. (1993) Differential function and expression of *Saccharomyces cerevisiae* B-type cyclins in mitosis and meiosis. *Mol Cell Biol*, **13**, 2113-2125.
4. Schwob, E., Bohm, T., Mendenhall, M.D. and Nasmyth, K. (1994) The B-type cyclin kinase inhibitor $p40^{SIC1}$ controls the G1 to S transition in *S. cerevisiae*. *Cell*, **79**, 233-244.
5. Chen, Y.K., Leng, C.H., Olivares, H., Lee, M.H., Chang, Y.C., Kung, W.M., Ti, S.C., Lo, Y.H., Wang, A.H., Chang, C.S. *et al.* (2004) Heterodimeric complexes of Hop2 and Mnd1 function with Dmc1 to promote meiotic homolog juxtaposition and strand assimilation. *Proc Natl Acad Sci U S A*, **101**, 10572-10577.
6. Herruzo, E., Ontoso, D., Gonzalez-Arranz, S., Cavero, S., Lechuga, A. and San-Segundo, P.A. (2016) The Pch2 AAA+ ATPase promotes phosphorylation of the Hop1 meiotic checkpoint adaptor in response to synaptonemal complex defects. *Nucleic Acids Res*, **44**, 7722-7741.
7. Lao, J.P., Cloud, V., Huang, C.C., Grubb, J., Thacker, D., Lee, C.Y., Dresser, M.E., Hunter, N. and Bishop, D.K. (2013) Meiotic crossover control by concerted action of Rad51-Dmc1 in homolog template bias and robust homeostatic regulation. *PLoS Genet*, **9**, e1003978.
8. Shinohara, A., Gasior, S., Ogawa, T., Kleckner, N. and Bishop, D.K. (1997) *Saccharomyces cerevisiae recA* homologues *RAD51* and *DMC1* have both distinct and overlapping roles in meiotic recombination. *Genes Cells*, **2**, 615-629.

9. Joshi, N., Barot, A., Jamison, C. and Borner, G.V. (2009) Pch2 links chromosome axis remodeling at future crossover sites and crossover distribution during yeast meiosis. *PLoS Genet*, **5**, e1000557.
10. Lo, Y.H., Chuang, C.N. and Wang, T.F. (2014) Pch2 prevents Mec1/Tel1-mediated Hop1 phosphorylation occurring independently of Red1 in budding yeast meiosis. *PLoS One*, **9**, e85687.
11. Bartel, P.L. and Fields, S. (1995) Analyzing protein-protein interactions using two-hybrid system. *Methods Enzymol*, **254**, 241-263.
12. Beranger, F., Aresta, S., de Gunzburg, J. and Camonis, J. (1997) Getting more from the two-hybrid system: N-terminal fusions to LexA are efficient and sensitive baits for two-hybrid studies. *Nucleic Acids Res*, **25**, 2035-2036.
13. Cheng, C.H., Lo, Y.H., Liang, S.S., Ti, S.C., Lin, F.M., Yeh, C.H., Huang, H.Y. and Wang, T.F. (2006) SUMO modifications control assembly of synaptonemal complex and polycomplex in meiosis of *Saccharomyces cerevisiae*. *Genes Dev*, **20**, 2067-2081.
14. Lin, F.M., Lai, Y.J., Shen, H.J., Cheng, Y.H. and Wang, T.F. (2010) Yeast axial-element protein, Red1, binds SUMO chains to promote meiotic interhomologue recombination and chromosome synapsis. *Embo J*, **29**, 586-596.